Use of a single xenon flash lamp for photoacoustic computed tomography of multiple-centimeter-thick biological tissue *ex vivo* and a whole mouse body *in vivo*

Terence T. W. Wong
Yong Zhou
Alejandro Garcia-Uribe
Lei Li
Konstantin Maslov
Li Lin
Lihong V. Wang

SPIE.

Use of a single xenon flash lamp for photoacoustic computed tomography of multiple-centimeter-thick biological tissue *ex vivo* and a whole mouse body *in vivo*

Terence T. W. Wong, Yong Zhou, Alejandro Garcia-Uribe, Lei Li, Konstantin Maslov, Li Lin, and Lihong V. Wang*
Washington University in St. Louis, Optical Imaging Laboratory, Department of Biomedical Engineering, One Brookings Drive, Saint Louis, Missouri 63130, United States

Abstract. While lasers have been commonly used as illumination sources in photoacoustic (PA) imaging, their high purchase and maintenance costs, as well as their bulkiness, have hindered the rapid clinical dissemination of PA imaging. With this in mind, we explore an alternative illumination source for PA tomography—a xenon flash lamp with high pulse energy and a microsecond pulse width. We demonstrate that, by using a single xenon flash lamp, we can image both a black latex cord placed in chicken breast tissue at a depth of up to 3.5 cm *ex vivo* and an entire mouse body *in vivo*. Our findings indicate that the xenon flash lamp, producing optical illumination that is safe for humans, can be potentially applied to human tissue imaging. © *2016 Society of Photo-Optical Instrumentation Engineers (SPIE)* [DOI: 10.1117/1.JBO.22.4.041003]

Keywords: photoacoustic tomography; photoacoustic computed tomography; xenon flash lamp; deep tissue imaging.

Paper 160575SSR received Aug. 24, 2016; accepted for publication Oct. 10, 2016; published online Oct. 24, 2016.

In recent years, photoacoustic tomography (PAT) has demonstrated its capability of providing noninvasive, real-time imaging of significant anatomical and physiological information and shows great potential to impact the clinical assessment and treatment of diseases.[1–3] In PAT, pulsed lasers have long been the typical sources of illumination. Their superior pulse energy and short pulse duration provide strong acoustic waves for sensitive detection and high image resolution.[4,5] However, other features of the laser, such as its spatial and temporal coherence, are often unnecessary for efficient photoacoustic (PA) wave generation. More importantly, lasers' high cost, maintenance fees, laborious maintenance procedures, and bulky sizes hinder the rapid development of PAT for clinical usage. Clearly, a cost-effective and compact alternative illumination source would benefit certain applications. To this end, researchers have investigated pulsed laser diodes (LDs),[6–9] light-emitting diodes (LEDs),[10,11] and xenon flash lamps.[12] Using pulsed LDs, Upputuri and Pramanik[9] have imaged a blood-filled tube in chicken breast tissue up to 2-cm deep. However, pulsed LDs are typically available only at wavelengths greater than 800 nm, which limits the choices of label-free absorption-based contrasts. Using LEDs, Adachi and Hoshimiya[10] have successfully imaged printed characters. However, modulated LEDs have a long pulse width, which limits the bandwidth of the acoustic signals.[4,5] Although Allen and Beard[11] have recently demonstrated that overdriving LEDs could provide a much shorter pulse width (200 ns), which improved the acoustic wideband, the pulse energy was only ~10 µJ. In comparison, a xenon flash lamp has a much wider spectrum, much higher pulse energy, and a sufficiently short pulse width. However, previous demonstrations by Kruger[12] used a xenon flash lamp with a

relatively long temporal pulse width of ~5 µs, which severely degraded the image resolution. Therefore, Kruger did not provide PA images. In this work, we revisited the flash lamp idea and demonstrated, for the first time, the use of a single xenon flash lamp with high pulse energy and short temporal pulse width for PA computed tomography (PACT) of both biologically mimicking phantoms or tissues *ex vivo* and an entire mouse body *in vivo*. Traditional pulsed laser-based PACT has been used for performance comparisons.
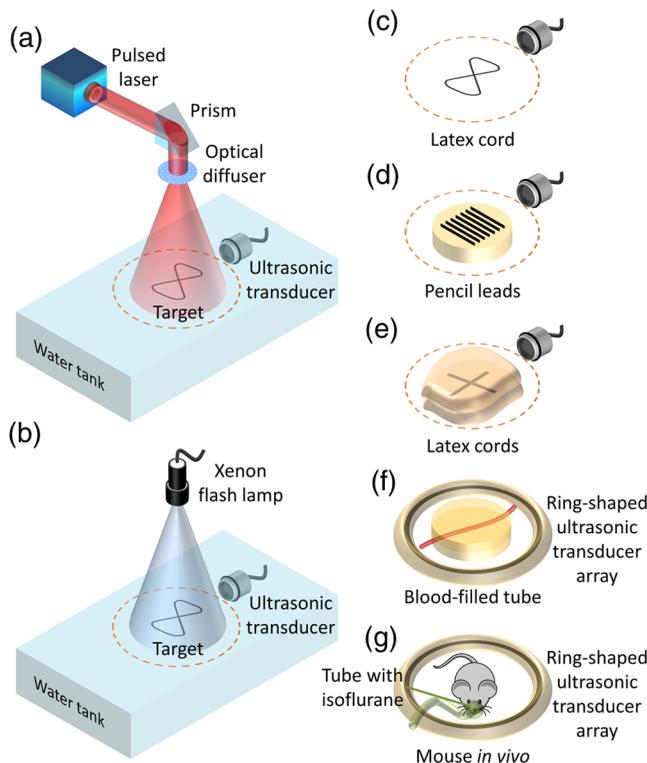
Figures 1(a) and 1(b) show schematics of our laser and flash lamp experimental setups, respectively. For laser illumination [Fig. 1(a)], we used a Q-switched Nd:YAG laser (Brilliant B, Quantel). The laser pulse energy was ~5 mJ, with an ~5-ns pulse width. The laser beam was reflected by a prism to illuminate the sample from the top. An optical diffuser homogenized and expanded the laser beam. For acoustic wave detection, a focused ultrasonic transducer (Olympus, 25.4-mm diameter and 25.4-mm focal length) was immersed in water on the same plane as the sample. The ultrasonic transducer was circularly scanned around the target in the trajectory shown by the orange dashed lines in Figs. 1(a)–1(e). The ultrasonic transducer was replaced by a ring-shaped ultrasonic transducer array with 512 elements to improve the signal-to-noise ratio (SNR) with more averaging and to avoid mechanical scanning for imaging fast dynamics [Figs. 1(f) and 1(g)].

For the xenon flash lamp setup [Fig. 1(b)], the optical system was simplified by directly illuminating the sample with the xenon flash lamp (L4634, Hamamatsu Photonics K. K.). The spectrum of the flash lamp light spanned from 240 to 2000 nm (Fig. 2). The repetition rate could be tuned from 10 to 100 Hz. The pulse energy was ~3 mJ with ~1-µs pulse width. The

---

divergence angle and output beam diameter were ~15 deg and ~2 cm, respectively. Thus, with 6-cm spacing between the lamp's output and the sample plane, the illumination light diverged enough to cover an imaging area of ~20 cm². Note that the circuit of the flash lamp was modified by externally adding two 0.1 μF capacitors in order to operate the flash lamp at its highest possible output. The American National Standards Institute (ANSI) maximum permissible exposure (MPE) on the skin surface is 20 mJ/cm² for the visible spectral range—covering most of the flash lamp spectrum, while the MPE is 3 mJ/cm² for the ultraviolet spectral range.[14] Nevertheless, the flash lamp fluence on the object surface is only ~0.15 mJ/cm². Therefore, flash lamp illumination is safe for human subjects and well within the ANSI safety limits.
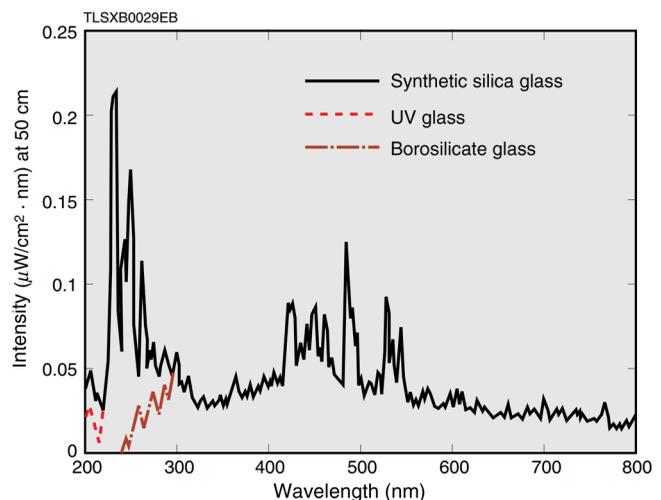
To reveal the potential of using a high-energy pulsed flash lamp as an alternative light source in PACT, two different latex phantoms, one pencil lead phantom, two blood-filled tube phantoms, and a live mouse were used: (i) a latex cord with a diameter of 1.5 mm, bent into the shape of the number "eight" [Fig. 1(c)], (ii) seven pencil leads with a diameter of 0.7 mm, laid on the surface of an agar–water gel [Fig. 1(d)], (iii) the same latex cords in a cross shape, sandwiched between pieces of chicken breast tissue [Fig. 1(e)], (iv) blood-filled tubes with a diameter of 1.5 mm, embedded 1-cm deep in an agar–water gel without and with a scattering medium [Fig. 1(f)], and (v) an entire mouse body *in vivo* [Fig. 1(g)].

First, to validate the feasibility of using a flash lamp in PACT, a latex cord [Figs. 1(c) and 3(a)] was imaged. The number "eight" shape enabled examining both the x- and y-axes' resolutions. To find the optimal ultrasonic transducer for xenon flash-lamp-based PACT, four focused ultrasonic transducers with varied center frequencies (0.5, 1.0, 3.5, and 5.0 MHz) were used to image the same phantom. The single-element ultrasonic transducers scanned around the phantom circularly in 400 steps. Figures 3(b)–3(e) show the reconstructed images acquired with flash lamp illumination (hereafter, referred to as flash-lamp-excited images) using the set of ultrasonic transducers. The flash-lamp-excited images acquired by 0.5- and 1.0-MHz ultrasonic transducers both show clear features of the phantom with high contrast. However, the other two images, acquired by 3.5- and 5.0-MHz ultrasonic transducers, are barely recognizable. A possible reason for this difference is that the pulse width of the flash lamp is relatively long (~1 μs), which limits the frequencies of PA signals less than 1 MHz. The contrast-to-noise ratio (CNR) was calculated as the mean of the enveloped PA amplitude in the region of interest (ROI) minus the mean of the enveloped background PA amplitude, divided by the standard deviation of the enveloped background PA amplitude, where the ROI is the target region. The CNRs for Figs. 3(b)–3(e) are 24.2, 22.2, 1.1, and 1.0, respectively. To better analyze the two images with high contrast, frequency spectra of the corresponding raw data are shown in Fig. 3(g). As shown by the frequency spectra, using a 1-MHz ultrasonic transducer provides only a slight resolution improvement over that achieved by using a 0.5-MHz transducer. This modest improvement was because the two data sets consist of similar frequency components, which were all <1 MHz. Therefore, to generate the flash-lamp-based PACT images with the highest CNR, the 0.5-MHz ultrasonic transducer is the best option.

By comparing the flash-lamp-excited and laser-excited images acquired with the same 0.5-MHz ultrasonic transducer [Figs. 3(b) and 3(f)], similar features can be observed, despite insignificant image blurring due to the long pulse width of the flash lamp. A spectral analysis was performed for further comparison between Figs. 3(b) and 3(f). As shown in Fig. 3(g), similar spectra can be observed, except for the frequency


Fig. 1 Schematics of the experimental setups and imaging targets. Experimental setups for (a) laser illumination and (b) xenon flash lamp illumination. Targets used in the experiments: (c) pure latex cord, (d) pencil leads laid on an agar–water gel, (e) latex cords sandwiched by pieces of chicken breast tissue with the same thickness, (f) blood-filled tube embedded in agar–water gel, and (g) a live mouse. The dashed circles in (a)–(e) represent the scanning trajectory of the ultrasonic transducer. A ring-shaped ultrasonic transducer array was used for targets (f) and (g).


Fig. 2 Spectra of the xenon flash lamp with various housings extracted from its specifications. Borosilicate glass is used for our flash lamp (Ref. 13, Hamamatsu Photonics K. K.).
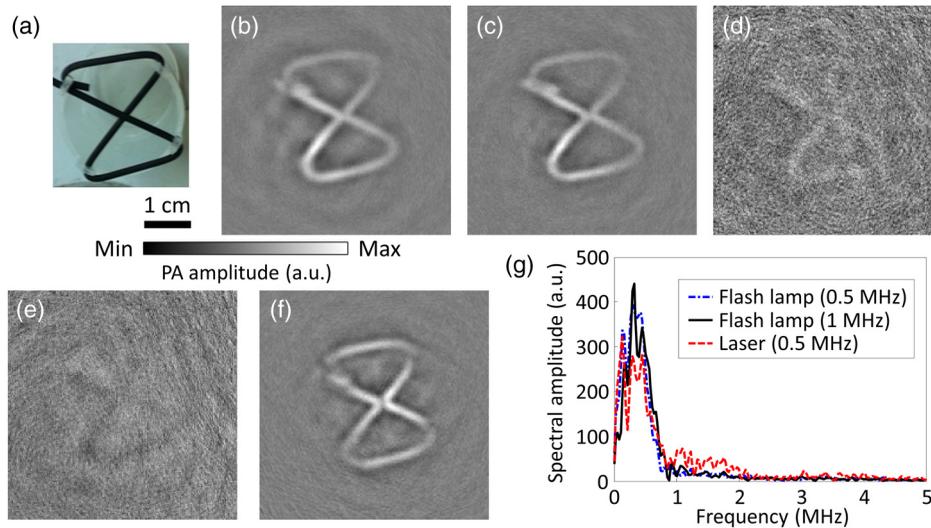
Fig. 3 PACT images and frequency spectra of the pure latex cord acquired using laser or xenon flash lamp illumination and ultrasonic transducers with varied center frequencies. (a) Photograph of the pure latex cord. PACT images acquired with flash lamp illumination and (b) 0.5, (c) 1.0, (d) 3.5, and (e) 5.0 MHz ultrasonic transducers. (f) PACT image acquired with laser illumination and the 0.5-MHz ultrasonic transducer. (g) Averaged frequency spectra of the raw PA signals acquired with the laser and flash lamp illumination.

components $\sim > 1$ MHz, where the relative (with respect to components < 1 MHz) spectral amplitude of the laser-acquired data is higher. Thus, with 0.5-MHz ultrasonic transducer acquisition, the quality of the image produced by flash lamp excitation is similar to that of the image produced by laser excitation. In the following experiments, we chose the 0.5-MHz focused ultrasonic transducer for all measurements.

To characterize the imaging resolution of xenon flash-lamp-based PACT, seven pencil leads were placed 6 mm apart atop an agar–water gel (3% agar), which held the pencil leads in place [Figs. 1(d) and 4(a)]. Laser-excited and flash-lamp-excited images are shown in Figs. 4(b) and 4(c), respectively. The imaging resolution was defined as the full-width-at-half-maximum of the reconstructed signals in the direction perpendicular to the
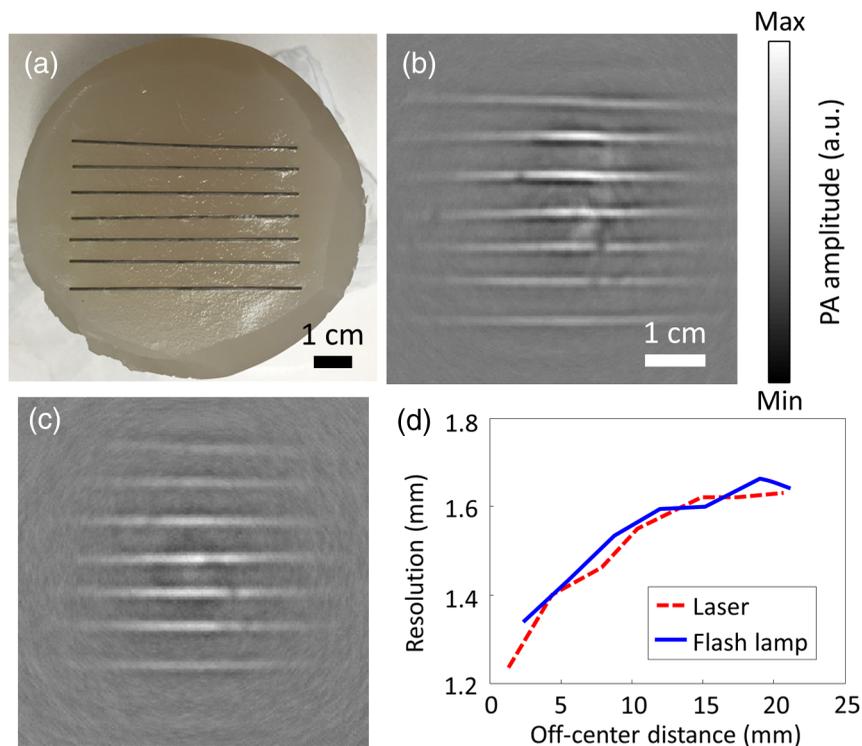
Fig. 4 PACT of a pencil lead phantom. (a) Photograph of the pencil lead phantom. PACT images acquired with (b) laser and (c) flash lamp illumination. (d) Plots of resolution versus the off-center distance of this line phantom.
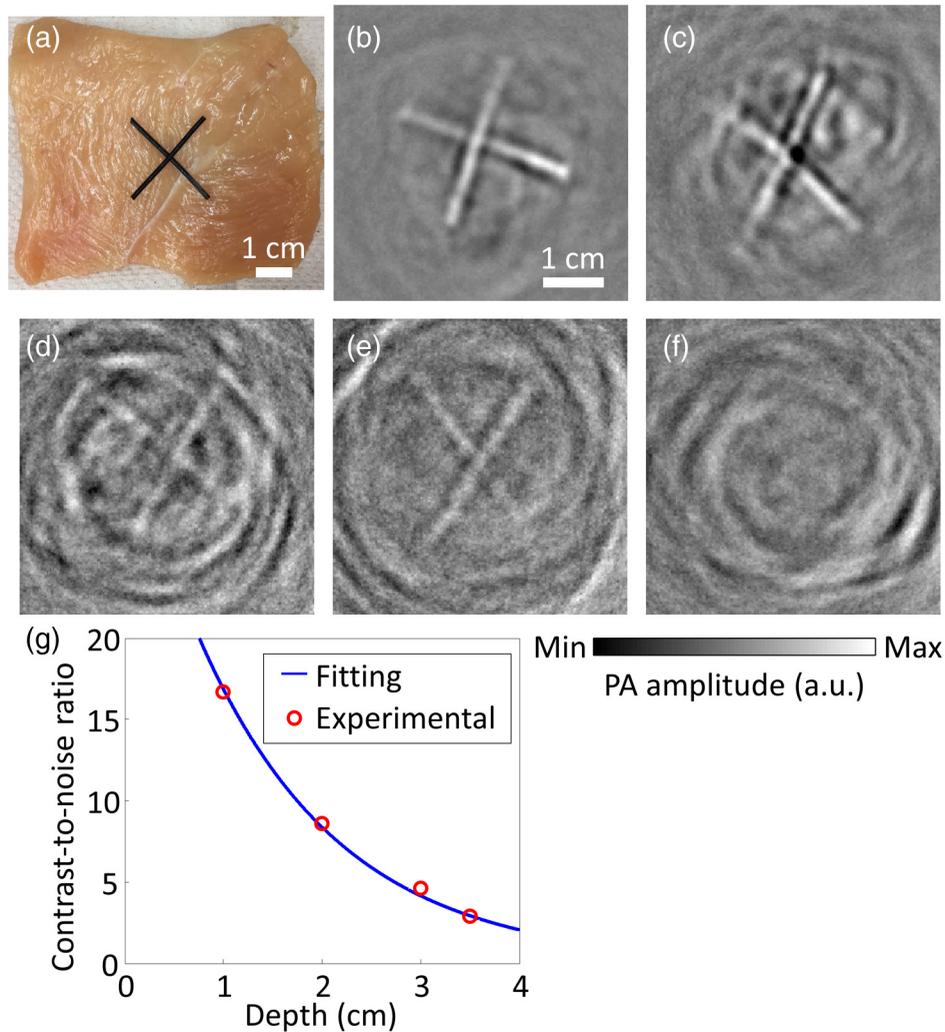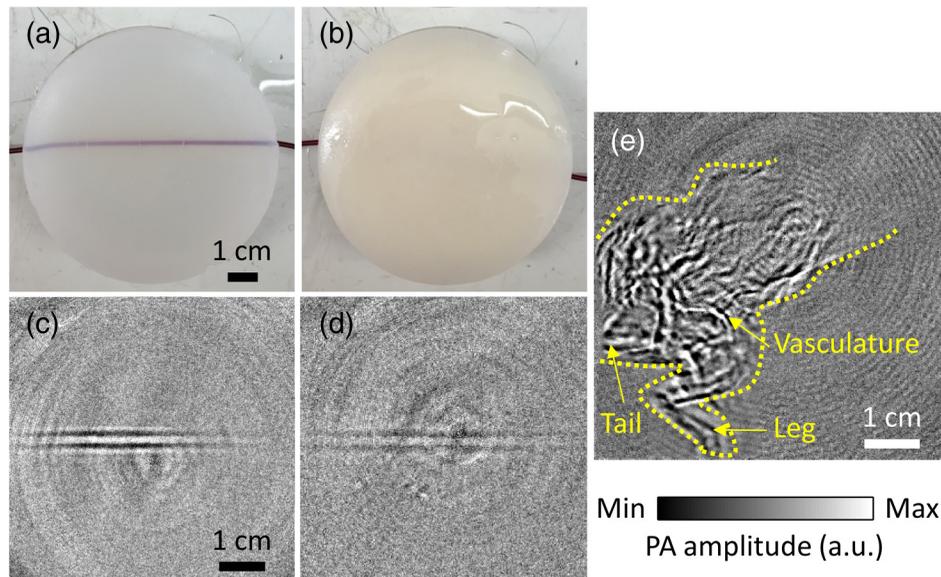
Fig. 5 Xenon flash-lamp-based PACT of tissue phantoms made of latex cords sandwiched by chicken breast tissue with varied preset thicknesses. (a) Photograph of an exposed phantom with the top chicken breast tissue removed. (b)–(f) PACT images of the phantoms. The surrounding chicken breast tissue had thicknesses of (b) 1.0, (c) 2.0, (d) 3.0, (e) 3.5, and (f) 4.0 cm. (g) Plot of CNR versus the depth of the latex cords, showing both experimental data points and best-fitting exponential decay curve.

pencil leads. Five adjacent line profiles perpendicular to the pencil leads were used to calculate the average imaging resolutions for both flash-lamp-excited and laser-excited images. Figure 4(d) plots their imaging resolutions versus their off-center distances. The two resolution plots overlap highly, showing that the short pulsed xenon flash lamp preserves the imaging resolution well. The average in-plane imaging resolution within the 25-mm radius area is ∼1.5 mm for both the laser-excited and flash-lamp-excited images.

To demonstrate the practicability of using a flash lamp for biomedical applications such as deep tissue imaging, we carried out another experiment to explore the maximum depth where a recognizable PA image can still be achieved. Here, we sandwiched two crossed latex cords [Fig. 1(e)] between pieces of chicken breast tissue, with the same thickness on the top, bottom, and sides. Figure 5(a) is a photograph of the phantom with the top pieces of chicken breast tissue removed. Note that the bottom and side chicken breast tissues were essential to prevent any stray light from bypassing the top chicken breast tissue and illuminating the latex cross via an unscattered path. Hence, no matter how the light traveled, it always traversed, at the least, the

preset thicknesses of chicken breast tissue. To determine the maximum penetration depth, chicken breast slices with different thicknesses (1.0, 2.0, 3.0, 3.5, and 4.0 cm) were used to sandwich the cross phantom. The corresponding reconstructed images are shown in Figs. 5(b)–5(f). Four times averaging was used to improve the SNR by a factor of 2 without significantly lengthening the scanning time. All the reconstructed images, except the image sandwiched by 4.0-cm thick chicken breast tissue, clearly show the cross structures, with different extents of artifacts. Artifacts around the cross structures can be suppressed by better sandwiching the latex cords to reduce air bubbles between the interfaces. The CNRs for Figs. 5(b)–5(e) are 16.7, 8.6, 4.6, and 2.9, respectively. As shown in Fig. 5(g), the best-fitting exponential decay curve proves that CNRs decay exponentially with penetration depths. Our experimental results supported that a single xenon flash lamp could achieve 3.5-cm deep tissue imaging of black latex cords with a CNR of around 2.9, which is enough for many biomedical applications, such as human breast cancer and skin melanoma imaging. Note that multiple flash lamps can be used to further improve the CNR and thus the penetration depth.

Fig. 6 Xenon flash-lamp-based PACT of blood-filled tube phantoms made by embedding blood-filled tubes at a depth of 1 cm inside an agar–water gel without and with a scattering medium, and a whole mouse body *in-vivo*. (a) and (b) Photographs of the blood-filled tube phantoms without and with 1% intralipid, respectively. (c) and (d) PACT images of the phantoms (a) and (b), respectively. (e) PACT image of the whole mouse body *in vivo*. Different structures, such as the vasculature, leg, and tail are labeled. The mouse body is also outlined with yellow dashed lines.

To demonstrate the full potential of flash-lamp-based PACT for blood imaging, we imaged blood-filled tubes, which were embedded 1-cm deep inside an agar–water gel (3%) without and with 1% intralipid [Figs. 1(f), 6(a), and 6(b)]. To image the blood, which is less absorbing than the latex cord, we replaced the single-element ultrasonic transducer with a ring-shaped ultrasonic transducer array with 512 elements to improve SNR by employing more averaging. In particular, 1000 times averaging was used to image the blood-filled tube. We can clearly see the blood-filled tube in the clear medium phantom from the flash-lamp-excited image [Fig. 6(c)]. The blood-filled tube can also be observed with sufficient contrast even inside the scattering medium at the same depth [Fig. 6(d)].

With, at the least, a 1-cm imaging depth for blood, we further imaged a whole mouse *in-vivo* [Fig. 1(g)] with 5000 times averaging. The mouse's body was completely immersed in water, but the head was above water so that the mouth could be connected to a tube supplying constant anesthetic gas (isoflurane). The flash-lamp-excited image is shown in Fig. 6(e), with a CNR of 21.7. We can easily recognize different structures of the mouse, including the vasculature in the body, legs, and tail. Note that mouse head was not imaged here because it was not immersed in water.

To conclude, we have demonstrated the feasibility of using a single xenon flash lamp as the illumination source for PACT. Taking CNR as the main concern, the optimal ultrasonic transducer for a xenon flash lamp was found to be a focused one with a center frequency of 0.5 MHz. The average in-plane imaging resolution was ~1.5 mm within the imaging field-of-view. Different phantoms were used for validation, and all of them showed promising results. Flash-lamp-excited images showed structures similar to those in the laser-excited images, and the demonstrated maximum penetration depth for imaging black latex cords was 3.5 cm in the chicken breast tissue, which is around one-half of the maximum penetration depth reported

by using lasers.[2] A blood-filled tube at a depth of 1 cm inside a scattering medium and a whole mouse body *in-vivo* can also be imaged with a single xenon flash lamp illumination, which can open up many cost-effective applications for flash-lamp-based PACT. Using a single xenon flash lamp with minimal optical and acoustic components, a complete PACT system can be appealingly compact and cheap, facilitating the usage of PAT in clinics and global healthcare. For example, with a safe xenon flash lamp, it may be possible to implement an inexpensive and portable PA handheld probe to detect skin melanoma[15] and breast tumor in humans.

References

1. L. V. Wang, "Multiscale photoacoustic microscopy and computed tomography," *Nat. Photonics* **3**(9), 503–509 (2009).
2. L. V. Wang and S. Hu, "Photoacoustic tomography: *in vivo* imaging from organelles to organs," *Science* **335**(6075), 1458–1462 (2012).
3. P. Beard, "Biomedical photoacoustic imaging," *Interface Focus* **1**(4), 602–631 (2011).
4. L. V. Wang, "Tutorial on photoacoustic microscopy and computed tomography," *IEEE J. Select. Topics Quantum Electron.* **14**(1), 171–179 (2008).
5. L. V. Wang and H. Wu, *Biomedical Optics: Principles and Imaging*, Wiley, Hoboken, New Jersey (2007).

6. T. J. Allen and P. C. Beard, "Pulsed near-infrared laser diode excitation system for biomedical photoacoustic imaging," *Opt. Lett.* **31**(23), 3462–3464 (2006).

7. L. Zeng et al., "Portable optical-resolution photoacoustic microscopy with a pulsed laser diode excitation," *Appl. Phys. Lett.* **102**, 053704 (2013).

8. R. G. M. Kolkman, W. Steenbergen, and T. G. van Leeuwen, "In vivo photoacoustic imaging of blood vessels with a pulsed laser diode," *Lasers Med. Sci.* **21**, 134–139 (2006).

9. P. K. Upputuri and M. Pramanik, "Performance characterization of low-cost, high-speed, portable pulsed laser diode photoacoustic tomography (PLD-PAT) system," *Biomed. Opt. Express* **6**, 4118–4129 (2015).

10. Y. Adachi and T. Hoshimiya, "Photoacoustic imaging with multiple-wavelength light-emitting diodes," *Jpn. J. Appl. Phys.* **52**, 07HB06 (2013).

11. T. J. Allen and P. C. Beard, "High power visible light emitting diodes as pulsed excitation sources for biomedical photoacoustics," *Biomed. Opt. Express* **7**, 1260–1270 (2016).

12. R. A. Kruger, "Photoacoustic ultrasound," *Med. Phys.* **21**(1), 127–131 (1994).

13. "Super-quiet xenon flash lamps," pp. 1–16, Hamamatsu Photonics K. K., Japan, https://www.hamamatsu.com/resources/pdf/etd/Xe-F_TLS1003E.pdf (2013).

14. *American National Standard for Safe Use of Lasers*, ANSI Standard Z136. 1–2000, Laser Institute of America, New York (2000).

15. Y. Zhou et al., "Handheld photoacoustic microscopy to detect melanoma depth *in vivo*," *Opt. Lett.* **39**(16), 4731–4734 (2014).

Terence T. W. Wong received his bachelor's and master's degrees from the University of Hong Kong in 2011 and 2013, respectively, under the supervision of Dr. Kevin Tsia. Currently, he is a graduate student in biomedical engineering at Washington University in St. Louis, under the supervision of Dr. Lihong V. Wang. His research focuses on both photoacoustic (PA) microscopy and tomography, especially on developing a low-cost PA imaging system for global healthcare and high-speed PA microscope for histology imaging.

Yong Zhou was a graduate student in biomedical engineering at Washington University in St. Louis, under the supervision of Dr. Lihong V. Wang, Gene K. Beare Distinguished Professor. His research focuses on the development of PA imaging systems.

Alejandro Garcia-Uribe received his MSc and PhD degrees in electrical engineering from the Department of Electrical and Computer Engineering, Texas A&M University, College Station. Currently, he is a research scientist at the Optical Imaging Laboratory, Department of Biomedical Engineering, Washington University in St. Louis. His research interests include optical imaging, biomedical optics, biomedical image analysis, and digital signal processing.

Lei Li received his bachelor's and master's degrees from Harbin Institute of Technology, China, in 2010 and 2012, respectively. Now, he is working as a graduate research assistant under the tutelage of Dr. Lihong Wang at Washington University. His current research focuses on PA microscopy and tomography, especially on improving PA imaging performance and applying it to brain functional imaging and small animal whole body imaging.

Konstantin Maslov graduated from Moscow Institute of Physics and Technology with a major in biophysics and received his PhD in physical acoustics from Moscow State University, Russia. After graduation, he worked at the Institute of Chemical Physics, Russian Academy of Sciences and Texas A&M University. Currently, he is a research associate professor at the Biomedical Engineering Department, Washington University in St Louis, Missouri. His area of interest includes optical, PA and acoustic imaging, and PA spectroscopy.

Li Lin received his master's degree from the University of Pennsylvania in 2013 and his bachelor's degree from Tianjin University in 2011. Currently, he is a PhD student at Washington University in St. Louis, under the tutelage of Dr. Lihong V. Wang. His research focuses on PA tomography and microscopy.

Lihong V. Wang: Biography is not available.